Taylor & Francis
Taylor & Francis Group

Biofouling
The Journal of Bioadhesion and Biofilm Research

ISSN: 0892-7014 (Print) 1029-2454 (Online) Journal homepage: www.tandfonline.com/journals/gbif20

Biofouling on aquaculture mesh: disentangling seasonal and environmental effects with DNA metabarcoding

Tian Tian, Xavier Pochon, Peter Bell & Maren Wellenreuther

To cite this article: Tian Tian, Xavier Pochon, Peter Bell & Maren Wellenreuther (15 Jun 2026): Biofouling on aquaculture mesh: disentangling seasonal and environmental effects with DNA metabarcoding, Biofouling, DOI: 10.1080/08927014.2026.2675243

To link to this article: https://doi.org/10.1080/08927014.2026.2675243

BIOFOULING
https://doi.org/10.1080/08927014.2026.2675243

Biofouling on aquaculture mesh: disentangling seasonal and environmental effects with DNA metabarcoding

Tian Tian[a,b], Xavier Pochon[c,d], Peter Bell[b] and Maren Wellenreuther[a,b]

[a]School of Biological Sciences, University of Auckland, Auckland, New Zealand; [b]Seafood Technologies, Bioeconomy Science Institute, Nelson, New Zealand; [c]Molecular Surveillance Team, Biosecurity Group, Cawthron Institute, Nelson, New Zealand; [d]Institute of Marine Science, University of Auckland, Auckland, New Zealand

ABSTRACT

Biofouling presents ecological and economic challenges for marine industries, yet patterns of community development in relevant environments remain underexplored. In this study, we investigated seasonal (winter vs. summer) and spatial (sheltered vs. exposed) patterns of eukaryotic biofouling across six coastal sites in New Zealand. Using standardised mesh substrates and DNA metabarcoding with the 18S rRNA gene, we characterised over 10,000 amplicon sequence variants (ASVs) across 216 samples, revealing 541 species from 249 taxonomic classes. Exposed sites exhibited marked seasonal contrasts: winter communities were dominated by hydroids (e.g. *Coryne eximia*), whereas summer assemblages were rich in amphipods (e.g. *Jassa slatteryi*). Sheltered sites showed more stable biomass and diversity but greater site-level variability, especially in summer. Temperature and wind fetch were strongly associated with community variation, with larger seasonal fluctuations observed under high-exposure conditions. Notably, several dominant species were non-native, underscoring the importance of early detection and tailored antifouling strategies.

ARTICLE HISTORY
Received 2 October 2025
Accepted 11 May 2026

KEYWORDS
Antifouling management; coastal environments; eukaryotic community; marine industry; metabarcoding

Introduction

Biofouling is a natural process in marine ecosystems but also represents one of the major challenges for marine-related industries, including maritime transport and shipping, aquaculture, and other coastal anthropogenic activities (Flemming et al. 2009; Fitridge et al. 2012). The accumulation of fouling organisms on artificial structures increases hydrodynamic drag, structural load, and maintenance costs, while also facilitating the spread of non-indigenous and harmful species (Dürr and Thomason 2009). In recent years, numerous antifouling tools have been developed and applied to mitigate biofouling impacts (Cao et al. 2011). However, the effectiveness and cost-efficiency of many of these tools remain uncertain, and some may pose pollution risks to marine ecosystems (Bannister et al. 2019). Furthermore, standardised management is difficult to achieve because biofouling communities vary strongly across environmental and seasonal conditions (Vinagre et al. 2020). These challenges indicate the pressing need for effective biofouling monitoring to guide comprehensive antifouling strategies and site-specific management.

Fine-scale monitoring of biofouling communities is essential to understand how the changing environments influence their presence, growth and to identify potentially problematic species. As such, resulting data can inform community modelling and future prediction, which facilitates targeted and efficient management (Bannister et al. 2019). Data composition analyses can further support the early detection of newly arrived species and provide insights into the factors potentially contributing to successional patterns. By tracking the presence and growth of key biofouling species, high-risk periods and locations for fouling can be predicted (Wu et al. 2023). This allows more specific approaches that ultimately deliver effective management actions, while reducing unnecessary treatments and environmental impacts. For example, biofouling monitoring can inform aquaculture site and farming season selection, enable long-

CONTACT Maren Wellenreuther Maren.Wellenreuther@plantandfood.co.nz

Supplemental data for this article can be accessed online at https://doi.org/10.1080/08927014.2026.2675243.

term modelling of harmful species distribution, and guide cleaning schedules and antifouling measures (Sylvester et al. 2011; Atalah et al. 2017).

Traditional biofouling monitoring has largely relied on visual assessments, biomass measurements, and morphological identification (Sievers et al. 2014; Wrange et al. 2020). While widely used, these approaches often provide limited taxonomic resolution and incur higher costs, particularly for cryptic, damaged, early-stage, or morphologically similar taxa, such as common invasive tunicates (e.g. *Ciona intestinalis*) and mussels (e.g. *Mytilus galloprovincialis*), whose juveniles are difficult to distinguish from other native species (Braby and Somero 2006; Zhan et al. 2015). Without high-resolution monitoring, these high-risk taxa may go undetected in the complex biofouling community, reducing antifouling effectiveness and increasing ecological and economic risks (Azevedo et al. 2020; de Souza et al. 2025).

Over the past two decades, high-throughput molecular tools, such as next generation sequencing (NGS) and DNA metabarcoding, have emerged as powerful complementary approaches for complex community analysis (Taberlet et al. 2012; Behjati and Tarpey 2013). By targeting standardised genetic markers, DNA metabarcoding enables the simultaneous identification of diverse taxa from bulk organisms or environmental samples and has been increasingly applied in biofouling research (Valentini et al. 2009; Ruppert et al. 2019). While methodological limitations such as sampling and experimental biases, and reference database coverage can influence taxonomic resolution and detection accuracy, DNA metabarcoding provides a robust and efficient framework for comparative analyses of biofouling communities across environmental gradients and industrial contexts. Despite its widespread use in ecological and environmental assessments of biofouling communities (Pochon et al. 2015; von Ammon et al. 2018; Pearman et al. 2021), applications in marine industry settings remain limited.

In this study, we used DNA metabarcoding of bulk biofouling organisms collected from standard industrial mesh to characterise eukaryotic biofouling communities across two seasons (winter and summer) and two wind exposure regimes (sheltered and exposed to open ocean) in New Zealand coastal waters. These regimes represent contrasting physical conditions typical of aquaculture and marine infrastructure, where temperature and wind-driven water motion strongly influence larval settlement, biomass accumulation, and community development (Koehl 2007). By combining biomass measurements with molecular analyses, we investigated both seasonal succession and monthly recruitment patterns. Our objectives were to: (1) assess biomass accumulation and alpha diversity across environmental gradients; (2) examine seasonal and spatial shifts in community composition and beta diversity; and (3) quantify and evaluate the effects of relevant environmental factors, particularly temperature and wind exposure. We hypothesised that biofouling dynamics would vary significantly with season and exposure, and that these insights could inform temporal cleaning schedules, spatial site selection, antifouling material deployment, and ultimately integrated mitigation strategies.

Materials and methods

Experimental design to characterise biofouling dynamics

To investigate seasonal and spatial patterns in biofouling community structure, we selected six sampling sites in the northern region of New Zealand's South Island. Three exposed sites located in Tasman Bay (E1–E3) and three sheltered sites in Pelorus Sound (S1–S3) served as replicates for the two exposure conditions (Figure 1(A)). Exposure in this context was determined by comparing relative differences in wind fetch between these sites, which was calculated by averaging the distances from the sampling site to the shores in all directions (Seers 2018). Sampling was conducted across two seasons, with winter spanning from June to September 2023 and summer from December 2023 to March 2024. Each site was sampled three times per season to capture both seasonal succession and monthly recruitment patterns.

Biofouling settlement was assessed using standardised material: 2.5 mm diameter Dyneema® mesh (knotted T90 square mesh, bar length = 33 mm, supplied by Hampidjan New Zealand Ltd), commonly used in marine industries. For each treatment, three replicate 10×10 cm mesh squares were attached to three small plastic inner frames with cable ties and mounted onto a 6×1 plastic array frame (manufactured by Nelson Plastics Ltd) (Figure 1(B,C)). For each site, four array frames were attached to a mooring line, including one for the monthly recruitment treatment (1.2 m below the sea surface) and three attached together for the seasonal succession treatment (15 cm below the monthly recruitment frame) (Figure 1(B,C)). The mooring lines were either bottom mounted with surface floats (exposed sites) or attached and hung from surface infrastructure

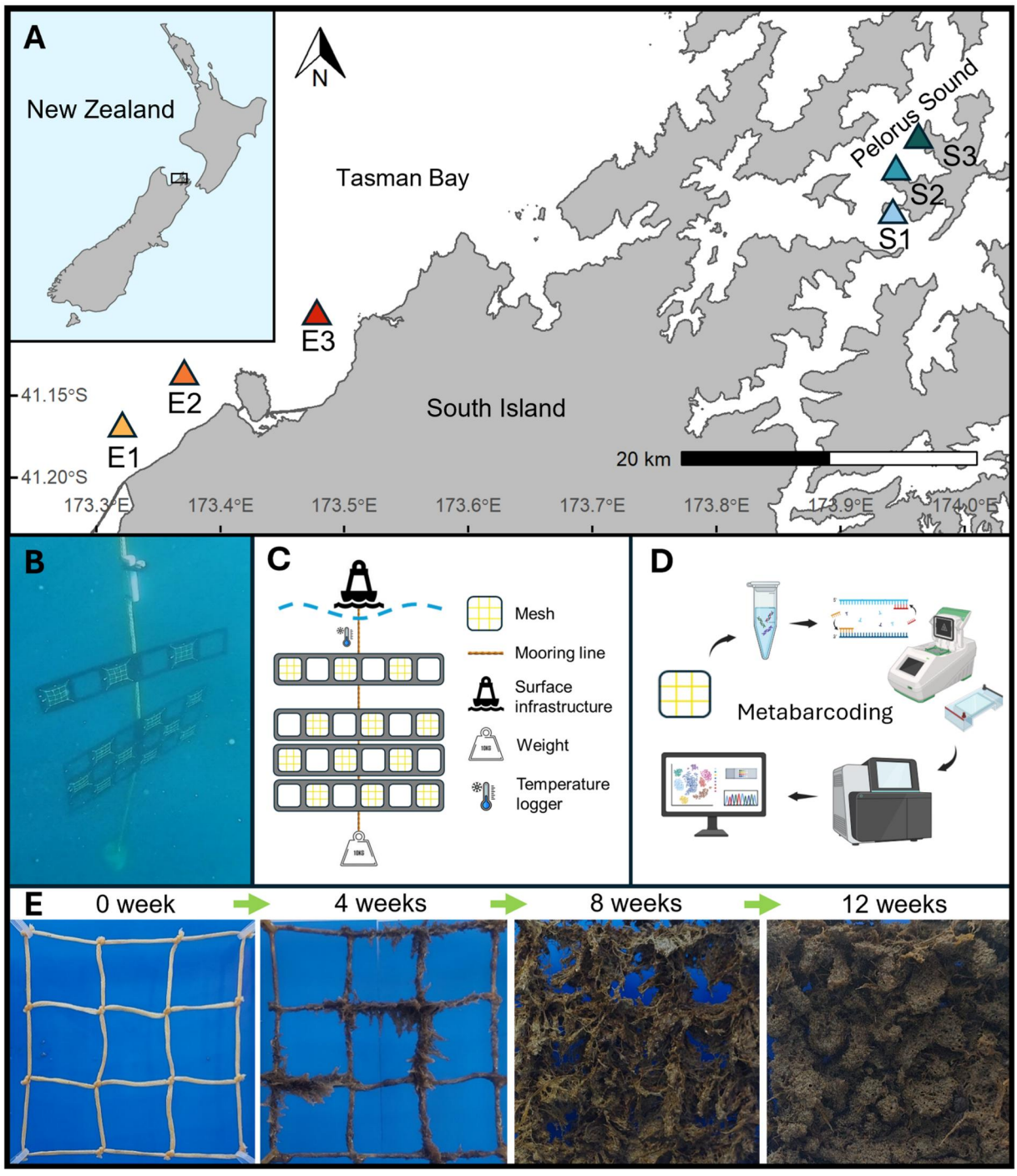

Figure 1. (A) Locations and sites where sampling was conducted: Tasman Bay (exposed sites E1-3) and Pelorus Sound (sheltered sites S1-3); (B) actual underwater image of deployed structures at S1; (C) sample deployment structure design with the 6 × 1 monthly recruitment panel and the 6 × 3 seasonal successional panel (ClipartMax 2018; Vecteezy 2025); (D) metabarcoding procedures (BioRender 2025); (E) seasonal succession samples at the initial deployment and at each sampling (0-12 weeks) at E1 in winter.

(sheltered sites). One environmental data logger (HOBO® Pendant Mx Temperature Logger, Onset, USA) was deployed under water at each site and set to record every 10 min. Metabarcoding preparations were performed after each sampling (Figure 1(D)). Samples were collected at intervals of 4, 8 and 12 weeks in each season (Figure 1(E)).

Sample collection, pre-processing and DNA extraction

During each sampling session, three monthly recruitment samples were collected from each site and immediately replaced with new meshes. In addition, three random samples from the seasonal succession frames were collected. At each site, a new and pre-

bleached mesh sample briefly exposed to ambient air (~2 min, to match the handling time of biofouling samples) was included as a negative control to monitor potential non-target DNA contamination (e.g. human DNA). Sterile gloves and 10% bleach solution were used throughout to minimise cross-contamination. The collected mesh samples were then stored in sterile 50 mL Falcon tubes (Item No. 227-261; Cellstar®, Greiner Bio-One, Austria) and kept on ice until transported to laboratory. Samples with large biomass were cut into separate pieces using sterile scissors and tweezers and stored in separate tubes before freeze drying, after which they were pooled again, and homogenised. Logger data were downloaded every sampling and loggers reset. In total, $n = 252$ samples were obtained, including 216 biofouling samples and 36 field negative controls.

Wet weight (WW) data were recorded immediately after samples arrived at the Plant & Food Research Institute (PFR) laboratory. Samples were then stored at −80 °C for at least 24 h before further processing. Freeze-drying (24–48 h at −57 °C; Gamma 1-16 LSC, Christ) and bead-beating (2 min at 1500 rpm; 1600 MiniG Spex SamplePrep) were used for sample homogenisation at the Cawthron Institute laboratory. Samples were then returned to the PFR laboratory for dry weight (DW) measurement. A subsample (100 mg) was taken from each 50 mL tube and transferred to a 5 mL PowerBead Pro tube (DNeasy PowerSoil Pro DNA Isolation Kit, QIAGEN, MOBIO, Carlsbad, USA), and DNA was extracted following the manufacturer's protocol. A negative extraction control (no biofouling organism) was included in every extraction run. DNA quality and quantity were assessed using a NanoDrop photometer (Implen Nanophotometer, Munich, Germany). Extracted DNA was stored in 50 µL elution buffer at −20 °C until library preparation.

Library preparation and high-throughput sequencing

The V4 region of the eukaryotic nuclear small-subunit ribosomal RNA (18S rRNA) gene was amplified by Polymerase Chain Reaction (PCR) using the primer set Uni18SF: 5′-AGG GCA AKY CTG GTG CCA GC-3′ and Uni 18SR: 5′-GRC GGT ATC TRA TCG YCT T-3′ (Zhan et al. 2013), with Illumina overhang adapters for dual indexing (Kozich et al. 2013). DNA samples were diluted (1:25 for 100–250 ng/µL; 1:50 for >250 ng/µL) to optimise amplification. PCRs were performed in a thermal cycler (Eppendorf® Mastercycler, Hamburg, Germany) in 50 µL reactions containing 25 µL 2× MyFi™ PCR Master Mix (Bioline Meridian Bioscience, USA), 2 µL of each primer (10 µM), 2 µL template DNA, and 19 µL double-distilled water (ddH_2O). Cycling conditions were 95 °C for 3 min; 37 cycles of 94 °C for 20 s, 54 °C for 20 s, and 72 °C for 30 s; and a final extension at 72 °C for 7 min (Audrézet et al. 2022). A PCR negative control (no DNA) was included in each PCR run. Amplicon quality was assessed on a subset of samples ($n = 66$) by gel electrophoresis. Amplicons were then purified and normalised (1-2 ng/µL) using SequalPrep normalisation plates (ThermoFisher Scientific, USA), and sequenced (2 × 300 bp) on an Illumina NextSeq™ platform at Sequench Ltd, Nelson, New Zealand). Raw sequence reads were deposited in the NCBI sequence read archive (SRA), under BioProject PRJNA1302565.

Bioinformatics and statistical analyses

Illumina overhang adapters were removed by the Nextseq™ platform following sequencing. Raw FASTQ files were demultiplexed and trimmed for primer removal (19 bp overlap) using CUTADAPT, version 4.9 (Martin 2011) in R. Quality filtering and denoising were followed by the parameters (truncLen = c(280,280), maxN = 0, maxEE = c(2,2), truncQ = 2) based on the read quality score analysed by the R package DADA2, version 1.26.0 (Callahan et al. 2016). Forward and reverse reads were merged with a minimum 10 bp overlap with no allowed mismatches. Chimeras were removed using the default 'consensus' method. Taxonomic assignment was conducted against the SILVA 18S rRNA reference database, 138.1 SSU Ref NR 99 (Yilmaz et al. 2014). Potential contaminations detected in negative controls were removed using the R package microDecon, version 1.0.2 (McKnight et al. 2019). Sequencing depth and diversity coverage were inspected via rarefaction curves generated by the 'ggrare' function from the R package ranacapa, version 0.1.0 (Kandlikar et al. 2018).

To characterise and quantify temporal and spatial variation in potentially relevant environmental factors, temperature trends were analysed from logger data, and wind fetch was calculated from site coordinates (Table S1), using the R package windfetch (version 2.1-1; Seers 2018). Wind fetch differences across exposure types were reported descriptively due to limited number of independent site replicates per exposure category ($n = 3$) and substantial within-site fetch

variations (Table S1). Temperature differences across seasons and exposure types were analysed using linear mixed-effects model (LMM) with Gaussian errors using the R package lme4, version 1.1.35.3 (Bates et al. 2015), including exposure and season as fixed categorical predictors with site as a random intercept to account for spatial pseudo-replication. Both variables were visualised with the R package ggplot2, version 3.3.6 (Wilkinson 2011).

Wet and dry weight data were visualised using boxplots in ggplot2. Alpha-diversity metrics (observed richness and Shannon index) were calculated from rarefied data (3241 reads/sample) using the R package phyloseq, version 1.40.0 (McMurdie and Holmes 2013). Biomass and alpha diversity were analysed with LMMs with lme4, including exposure and season as fixed categorical predictors, deployment length (4, 8, 12 weeks) as a categorical variable, and all two-way interactions, with site as a random intercept to account for spatial pseudo-replication. Collinearity among variables was assessed using Variance Inflation Factor (VIF) implemented in the R package car, version 3.1.2 (Fox and Weisberg 2019). High collinearity (VIF $>$ 5) was detected between exposure and wind fetch (VIF $\approx$ 56.4) and between season and temperature (VIF $\approx$ 5.2); therefore, only one variable from each correlated pair was retained in the models. Model selection used likelihood ratio tests and AIC (Akaike Information Criterion) comparisons (Akaike 1998; Burnham and Anderson 2002); two-way interaction models were retained for interpretability and parsimony despite slightly higher AIC than three-way models (ΔAIC $<$ 19.65). Model assumptions were checked with simulation-based residual diagnostics to check normality, homoscedasticity, and absence of outliers using the R package DHARMa, version 0.4.7 (Hartig 2025). Post-hoc pairwise comparisons were conducted using Tukey-adjusted estimated marginal means in the R package emmeans, version 1.11.2 (Lenth 2025).

Community composition was analysed on unrarefied, normalised proportional data using phyloseq and visualised with stacked bar plots using ggplot2 and the R package khroma, version 1.16.0 for colour palettes (Frerebeau 2025). The classes of the most abundant 50 species were selected for plotting as representative taxonomic groups. Community composition and replicate consistency were assessed using hierarchical clustering and multivariate statistics (see Figure S1 for details). Non-native species were identified based on the latest 161 species listed by Biosecurity New Zealand using the pest alert tool, applying a minimum sequence identity of 99.4% and a minimum sequence length of 400 bp (Zaiko et al. 2023).

Beta-diversity was analysed to assess the effects of seasonal and environmental factors on community composition (Whittaker 1960). Two-way PERMANOVA on rarefied data was used to test the effects of the two factors (e.g. season and exposure for seasonal succession patterns, temperature and wind fetch for monthly recruitment patterns) and their interactions. The function 'adonis_pq' (permutations = 999, method = 'bray', by = 'terms') from the R package MiscMetabar (Taudière 2023) was used for phyloseq objects, based on the 'adonis2' function from the R package vegan, version 2.7-1 (Oksanen et al. 2025). Homogeneity was tested for the factors' interactions with permutation of dispersions (PERMDISP) (assumption was met if $p > 0.05$) using the 'betadisper' function; if violated, analysis of similarities (ANOSIM) was applied (Clarke and Green 1988). *Post-hoc* pairwise comparisons were conducted using the R package pairwise Adonis, version 0.4 (Martinez 2020). Rarefied data were visualised using non-metric multidimensional scaling (NMDS) plots with Bray-Curtis dissimilarity distances across the two main factors (Kruskal 1964).

Results

All amplicons tested by gel electrophoresis had clear target bands (~600 bp). Close double bands were observed in some amplicons, a pattern commonly seen in samples with multiple species and amplified by universal primers with low specificity. No visible bands were found in negative controls. The raw sequencing yield of the 216 amplicons (negative controls excluded) was 32,486,494 sequence reads (mean 150,400 per amplicon). After data filtering, 21,309,064 reads remained (mean 98,653 per amplicon). Negative controls contained 5.42% of total raw reads, including five identified classes (Hydrozoa, Malacostraca, Aspergillaceae, Malasseziaceae, Magnoliopsida) and four identified species (*Obelia geniculata*, *Coryne eximia*, *Jassa slatteryi*, *Brassica oleracea*). Decontamination removed 1,155,313 reads (5.40% of total reads after filtering) and 61 amplicon sequence variants (ASVs), resulting in 20,153,751 retained reads (mean 93,304 per amplicon) representing 10,153 ASVs, with no detectable change in treatment-level community patterns. One amplicon (monthly recruitment) with no reads was excluded for the downstream analysis and did not affect treatment balance.

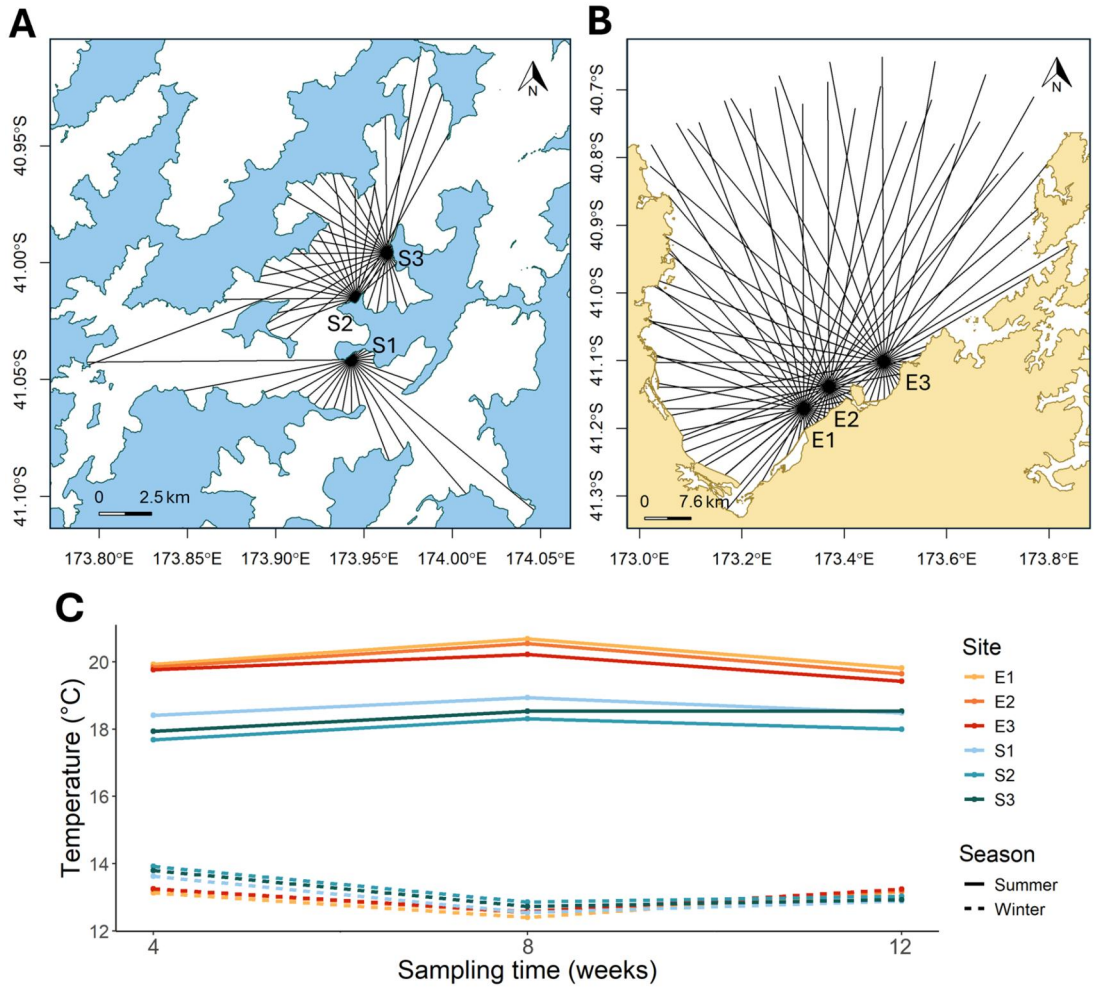

Figure 2. (A) Visualised wind fetch (distances from the site to the coasts in all directions) of each sheltered site; (B) visualised wind fetch of each exposed site; (C) line graph of the average monthly water temperatures at each site (displayed in different colours) at each sampling point in summer and winter (displayed in different line types).

The full list of the read counts per sample at each filtering and decontamination step is provided in Table S2.

Characterisation of wind fetch and temperature changes

Average wind fetches at exposed sites (78,674.24 m at E1, 80,482.00 m at E2, 80,600.62 m at E3) were about 40-fold higher than at sheltered sites (2,535.90 m at S1, 2,450.51 m at S2, 3,336.66 m at S3) (Figure 2(A,B)). Within each exposure type, wind fetch was similar among sites (descriptive statistics only, $n = 3$ per group, mean ± SE reported in Table S1), indicating no meaningful differences within the same exposure type (Figure 2(A,B)). Summer temperatures were significantly higher than winter temperatures at both exposures ($p < 0.01$), and within summer, exposed sites (20.05 ± 0.63 °C) were significantly warmer than sheltered sites (18.31 ± 0.63 °C; $p < 0.01$) (Figure 2(C)). In winter, temperatures did not differ significantly between exposure types ($13.24\,°C \pm 0.67$ °C for exposed sites and $12.84\,°C \pm 0.43$ °C for sheltered sites; $p = 0.12$) (Figure 2(C)). The full lists of temperature and wind fetch calculations, and LMM results are provided in Table S1.

Biomass and alpha diversity to measure seasonal accumulation patterns

WW and DW accumulation patterns at exposed sites differed significantly between summer and winter ($p = 0.01$ for WW; $p < 0.01$ for DW), whereas sheltered sites showed similar seasonal patterns ($p > 0.46$ for both WW and DW) (Figure 3(A,B)). At exposed sites, biomass accumulated faster and more continuously in winter, especially early in the season, with significantly higher quantities at 8 and 12 weeks compared to 4 weeks ($p < 0.01$ for both WW and DW) (Figure 3(A,B)). In summer, biomass fluctuated at exposed sites, with

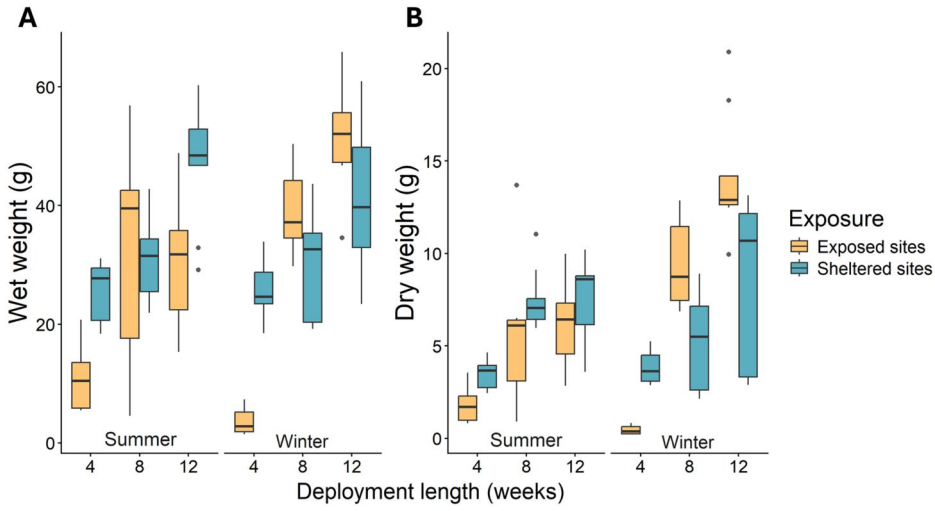

Figure 3. Boxplots showing wet weight (A) and dry weight (B) of seasonal succession samples from sheltered and exposed sites during summer and winter, across 4, 8 and 12 weeks of deployment. Boxes show the interquartile range, whiskers indicate the data range excluding outliers, and points represent outliers.

significant increases from week 4–8 ($p < 0.01$ for both WW and DW) and non-significant changes from week 8–12 ($p > 0.64$ for both WW and DW) (Figure 3(A,B)). Pronounced initial increases followed by subsequent declines at E1 and E3 were observed (Figure S2A). In contrast, sheltered sites exhibited slower biomass accumulation from week 4 to 8 in both seasons ($p > 0.08$ for both WW and DW except for DW in summer), followed by gradual yet significant increases ($p < 0.01$ for both WW and DW). During the first four weeks post-deployment, biomass was higher at sheltered sites than exposed sites ($p < 0.01$ for WW; $p = 0.01$ for DW). Overall, summer biomass was higher at sheltered sites ($p = 0.02$ for WW; $p = 0.24$ for DW), whereas winter differences were non-significant ($p > 0.16$ for both WW and DW). Random site effects were minor compared to residual variation, showing that most variability occurred within rather than among sites (6.17 vs. 79.34 for WW; 1.53 vs. 5.70 for DW). The full lists of LMM results and post-hoc pairwise comparisons of biomass are provided in Table S3.

Observed richness was higher at sheltered sites than exposed sites in both seasons ($p < 0.02$), especially in summer ($p < 0.01$) (Figure 4(A)). Seasonal differences within the same exposure were smaller but remained significant ($p < 0.05$) (Figure 4(A)). Significant increases were detected between weeks 4 and 12 at exposed sites in summer ($p = 0.01$), and between weeks 4 and longer deployments at sheltered sites in both seasons ($p < 0.01$) (Figure 4(A)). For Shannon index, growing patterns were similar at sheltered sites in both seasons and exposed sites in summer ($p > 0.06$), except for a drop at S1 at week 8 in summer (Figure S3B). In winter, a 7-fold growth increase was observed at two exposed sites (E1 & E3, Figure S3B) between weeks 4 and 12, ranging from 0.38 to 2.64. The full lists of LMM results and post-hoc pairwise comparisons of alpha diversity are provided in Table S4.

Biofouling community composition analyses to investigate seasonal dynamics

The most abundant 50 ASVs were assigned to 13 classes and 22 species, with two classes accounting for more than 50% of the total reads (29.83% of Malacostraca and 36.38% of Hydrozoa) (Table S5). Strong seasonal patterns were found at exposed sites, with Oligohymenophorea (26.85% of the total reads from exposed sites in summer), Copepoda (17.01%, mainly including 13.55% of *Harpacticus* sp. and 3.13% of *Temora turbinata*) and Malacostraca (46.43%, including 35.78% of *Jassa slatteryi*, 5.25% of *Jassa falcata* and 5.40% of *Caprella equilibra*) dominated in summer, whereas Hydrozoa (76.72%, including 52.54% of *Coryne eximia* and 24.18% of *Obelia geniculata*) and Malacostraca (13.47%, mainly including 6.80% of *Jassa slatteryi* and 6.49% of *Cyclograpsus cinereus*) dominated in winter (Figure 5). A clearer successional trend was observed at exposed sites in summer compared to winter. In summer, Gastropoda and Malacostraca decreased from weeks 4 and 8, while Copepoda increased from week 8 at all three sites (Figure 5). Comparatively, Hydrozoans remained dominant throughout winter at all three exposed sites,

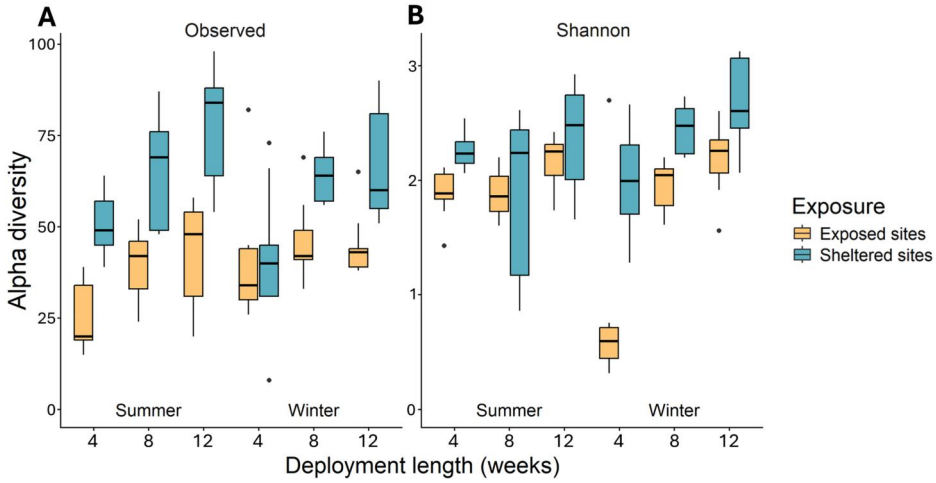

Figure 4. Boxplots showing observed richness (A) and Shannon diversity (B) of seasonal succession samples from sheltered and exposed sites during summer and winter, across 4, 8 and 12 weeks of deployment. Boxes show the interquartile range, whiskers indicate the data range excluding outliers, and points represent outliers.

with only small changes in Malacostraca and other classes (Figure 5).

Although the seasonal patterns were less pronounced at sheltered sites, distinct site differences were observed, especially in summer, with Hexacorallia (*Viatrix globulifera* at 69.22%) dominant at S1 (Figure 5). Relatively similar seasonal patterns were found at S2 and S3. Hydrozoa (32.09–42.82%, including *Obelia geniculata* at 24.42–38.49% and *Coryne eximia* at 4.33–7.67% for both seasons) grew rapidly in the first 4 weeks, then reduced from week 8, and Malacostraca (32.45–42.61%, including *Jassa slatteryi* at 20.76–26.57% and *Caprella equilibra* at 11.69–16.04% for both seasons) and Rhabditophora (22.81% and 5.36% of *Notoplana australis* in summer and winter, respectively) appeared from weeks 4 and 8 until week 12 in both seasons (Figure 5). In winter, more Hydrozoa species were detected at S1 than the other two sheltered sites from week 8, and both Ulvophyceae and Copepoda were observed during the first 4 weeks at S1 and S2 (Figure 5). The read counts and percentages of the classes and species from both seasons and locations are provided in Table S5.

All detected non-native ASVs were assigned to nine species, with *Jassa slatteryi* (23.72% of the total non-native reads), *Obelia geniculate* (34.84%) and *Coryne eximia* (41.44%) being the most abundant. Consistent with the full community compositions above, strong seasonal patterns in non-native species were found at exposed sites, with 98.26% of reads in summer were assigned to *Jassa slatteryi*, whereas 93.28% of reads in winter were assigned to Hydrozoan (*Obelia geniculata* at 18.82% and *Coryne eximia* at 74.46%) (Figure 6). Seasonal variation in non-native composition was less pronounced at sheltered sites. Nevertheless, *Jassa slatteryi* was more prevalent in summer, particularly at S1 and S2, while *Obelia geniculata* was more common in winter. Additionally, *Cladophora ruchingeri* occurred at low abundance from week 8 in summer and weeks 4 and 12 in winter at S1 and S2 (Figure 6). The read counts and percentages of the non-native species from both seasons and locations are provided in Table S6.

Beta diversity to assess seasonal and environmental effects on succession and recruitment patterns

Both season and exposure, and their interaction had significant effects on seasonal succession patterns of community composition (ANOSIM, $p < 0.01$ for all terms). Summer communities at exposed sites were significantly isolated from other treatments ($p < 0.01$), whereas exposed winter and sheltered communities clustered more closely but remained significantly different across sites and sampling points ($p < 0.01$) (Figure 7). Furthermore, significant seasonal succession trends were found in both seasons and exposures ($p < 0.05$), except between weeks 8 and 12 at sheltered sites ($p = 0.41$) and between weeks 4 and 8 at exposed sites ($p = 0.14$) in summer (Figure 7). Site-level differences within the same season and exposure were also observed, with E3 differing from E1 and E2 ($p < 0.01$), and S1 differing from S2 and S3 ($p < 0.01$) in summer (Figure 7). The full lists of ANOSIM and *post-hoc* pairwise comparison results of the successional beta diversity matrix are provided in Table S7.

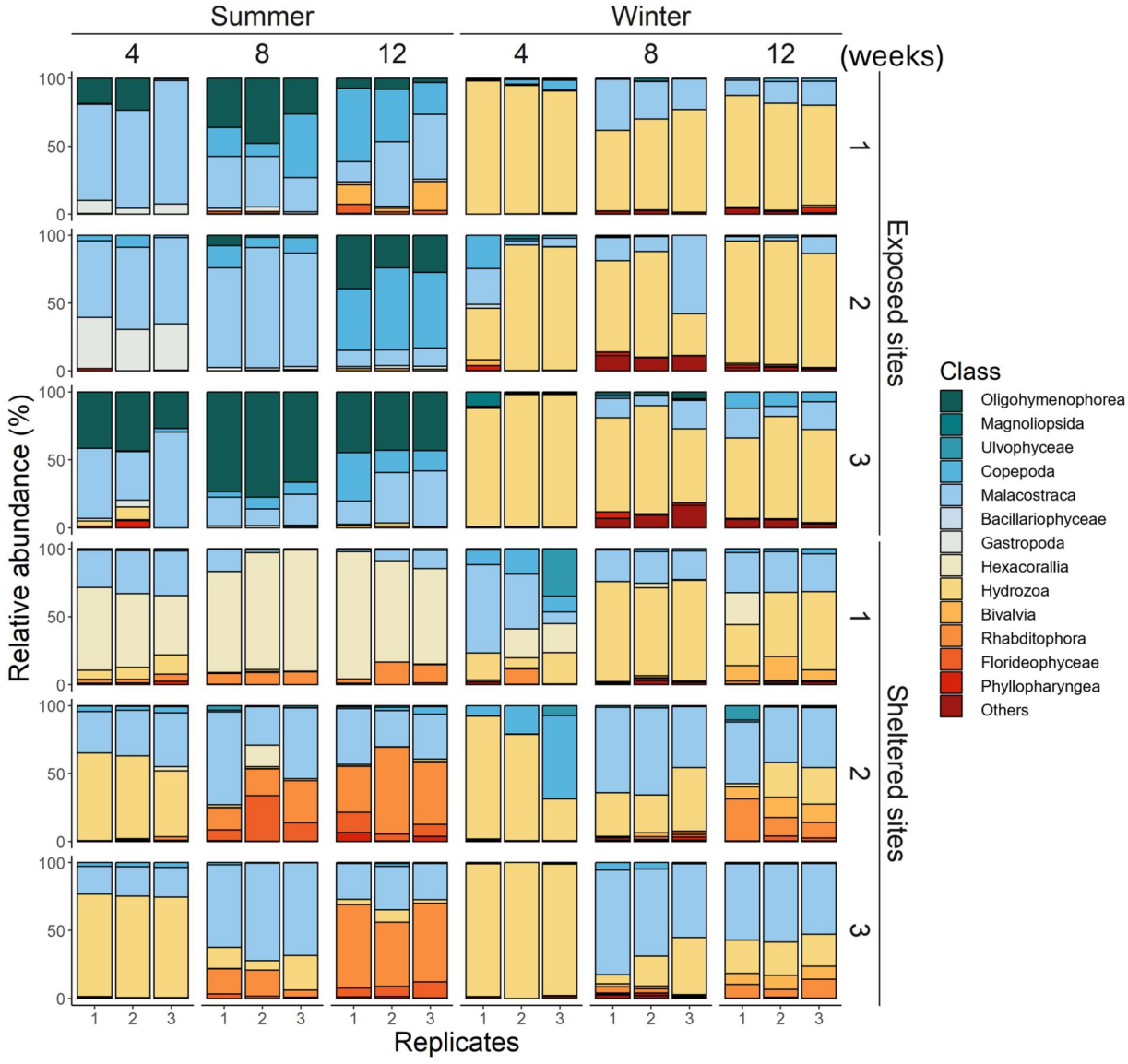

Figure 5. Relative abundances (%) of the most abundant 50 ASVs (displayed at class taxonomy level in different colours) from the seasonal succession samples at the sites of the two exposures in summer and winter (weeks 4 to 12), respectively. The three replicates of each treatment were displayed together.

Similarly, both temperature and wind fetch and their interaction had significant effects on monthly recruitment patterns (PERMANOVA, $p < 0.01$ for all terms). Community composition differed significantly between temperature levels and between wind fetch levels ($p < 0.01$), with greater seasonal separation at high wind fetch sites (Figure 8). Site-level variation within wind fetch levels was also observed ($p < 0.01$ for S1 vs. S2 & S3; $p < 0.02$ for E2 vs. E1 & E3) (Figure 8). Monthly shifts were significant across most temperature-wind fetch combinations ($p < 0.01$, except between weeks 4 and 8 at exposed sites in summer with $p = 0.19$, between weeks 8 and 12 at sheltered sites in summer with $p = 0.52$, and between weeks 8 and 12 at exposed sites in winter with $p = 0.09$) (Figure 8). The dispersion patterns within each season-exposure group reflected that wind explained more beta diversity at exposed sites across both seasons, whereas temperature had a strong influence in summer at exposed sites. Neither wind nor temperature showed strong associations with sheltered sites, and the absence of such an association was particularly pronounced in winter (Figure 8). The full lists of PERMANOVA and *post-hoc* pairwise comparison results of the monthly recruitment beta diversity matrix are provided in Table S8.

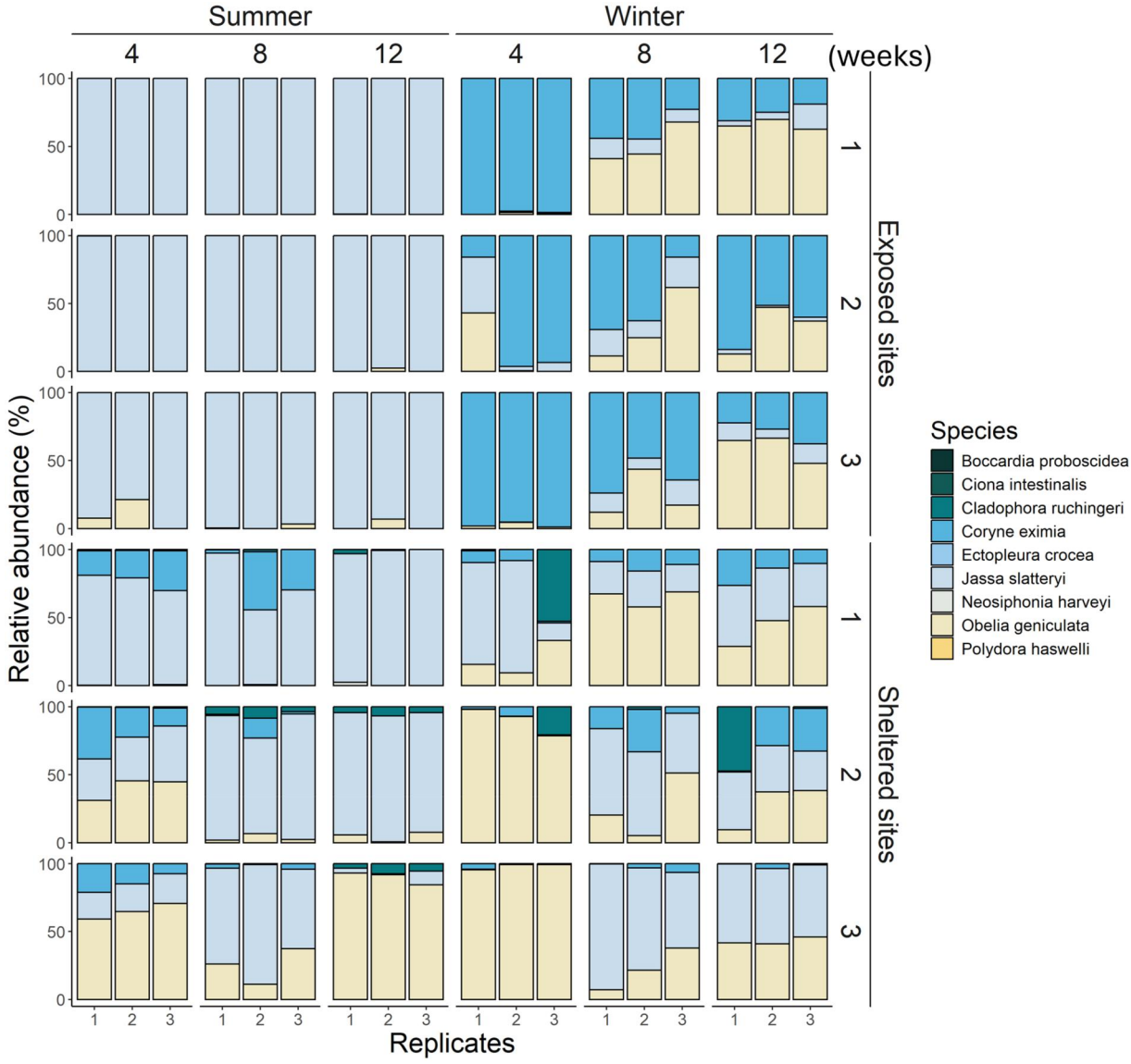

Figure 6. Relative abundances (%) of all the detected non-native species (displayed at species taxonomy level in different colours) from the seasonal succession samples at the sites of the two exposures in summer and winter (weeks 4 to 12), respectively. The three replicates of each treatment were displayed together.

Discussion

Biomass and diversity

In this study, strong seasonal and spatial variations were observed in biomass and diversity of eukaryotic biofouling, with temperature and wind exposure identified as important environmental factors associated with community patterns. As exposed sites were in Tasman Bay and sheltered sites in Pelorus Sound, exposure is partly confounded with regional setting; thus, observed patterns should be interpreted as associative, with potential contributions from other region-specific factors. Temperature and seasonal effects have been shown to influence fouling communities (Lord 2017; Ulaski and Konar 2024), while wave exposure and spatial location also play a key role in shaping assemblages (Garner and Litvaitis 2013; Visch et al. 2020). At exposed sites, wind appeared to strongly affect beta diversity in both seasons, with temperature exerting an additional influence during summer. In contrast, community composition at sheltered sites showed weak correlations with either wind or temperature, suggesting that other factors, such as nutrient availability, larval supply, and tidal influences, may play a greater role (Watts et al. 2015). These factors together provide a framework to interpret the observed patterns.

Higher water temperatures and lower exposure are generally expected to accelerate biomass growth (Atalah et al. 2016; Khosravi et al. 2019). However, we found

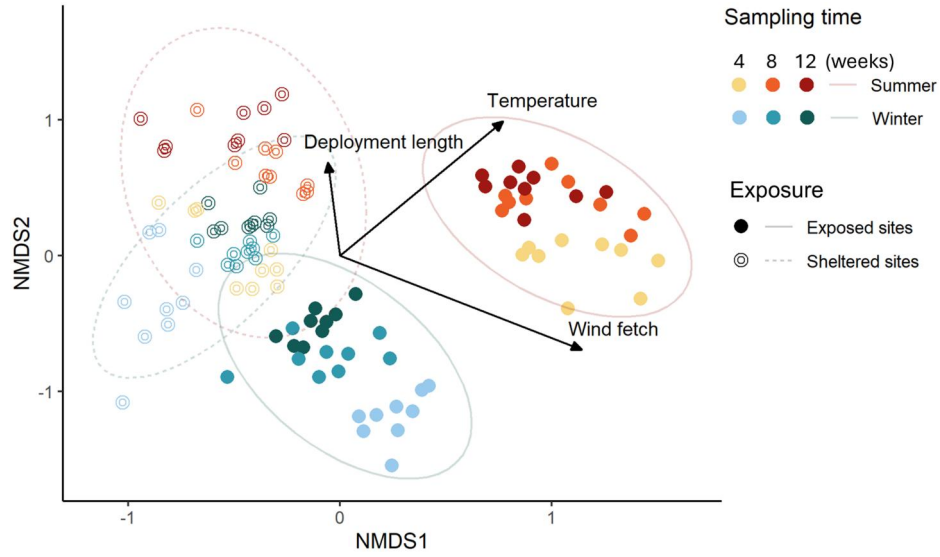

Figure 7. Non-metric multidimensional scaling (NMDS) plot of the seasonal succession samples at two exposures (displayed in different shapes) in summer and winter (weeks 4 to 12, displayed in warm colours for summer and cold colours for winter), respectively.

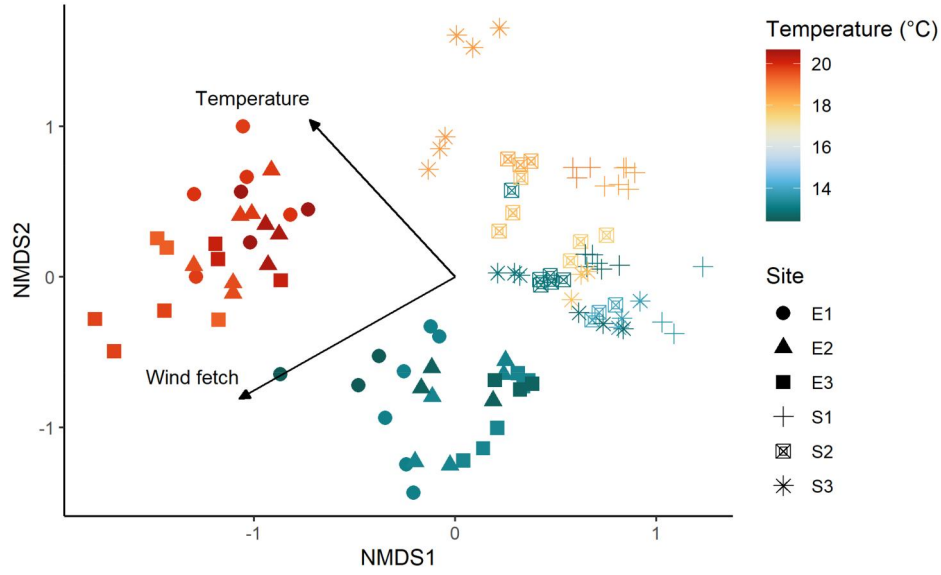

Figure 8. Non-metric multidimensional scaling (NMDS) plot of monthly recruitment samples from the six sampling sites, with sites represented by different shapes and seasonal temperature variation shown using a continuous colour gradient. Wind fetch differed significantly between the two exposure categories and was therefore represented by sheltered and exposed site groupings. Communities are shown for summer and winter monthly recruitment samples.

higher biomass and faster community development in colder and more exposed areas, indicating potential underlying factors. A previous biofilm study reported lower bacterial species richness in summer compared to winter, which may reduce settlement cues and subsequently limit eukaryotic recruitment (Chan et al. 2003). A similar phenomenon was noticed through visual observation in this study, where larger quantities of biofilm formed at exposed sites during winter, before the growth of the eukaryotic fouling community. To explain the reduction in WW/DW at exposed sites over summer, it was noted that amphipod-dominated communities were not tightly bound to the mesh and could be readily dislodged by increases in water flow or disturbances by marine animals. This was not observed among the more deeply 'rooted' hydroid-dominated communities in winter. In contrast, sheltered sites had more stable seasonal patterns, with similar biomass and

slightly higher genetic diversity than exposed sites. These findings suggest that marine environments with greater seasonal variability, such as fluctuations in temperature and water movement, tend to exhibit more pronounced seasonal differences in biofouling patterns.

Community composition

Most of the heavy and dense biomass at exposed sites during winter was attributed to ASVs assigned to two hydroid species *Obelia geniculata* and *Coryne eximia*, whereas summer communities were dominated by ASVs assigned to two amphipod species *Jassa slatteryi* and *Jassa falcata*. Previous studies suggest that the biomass accumulation and reproductive activities of hydroid species typically increase with rising summer temperatures (Puce et al. 2003; Slobodov and Marfenin 2004; Park and Hwang 2012). The enhanced hydroid growth observed in winter may be related to their strong adhesive capabilities and early biofilm formation (Hadfield 2011), together with increased water movement at exposed sites during this season, which can enhance nutrient flux and food delivery (Chiswell et al. 2021). These hydroid species add structural complexity to underwater substrates providing habitat and food for small invertebrates, such as crabs (*Cyclograpsus cinereus*), which were frequently and exclusively found at exposed sites in winter in this study. Comparatively, the soft and tubular structures constructed by amphipods using debris from biological and non-biological materials do not provide the same degree of habitat complexity (Beermann and Franke 2012).

Although seasonal differences at sheltered sites were less pronounced than at exposed sites, a greater diversity was detected, including ASVs assigned to algae such as *Cladophora ruchingeri* and *Polysiphonia* sp. Also, strong site differences were detected at sheltered sites especially in summer. The dominant ASVs assigned to anemone *Viatrix globulifera* and caprellid *Caprella equilibra* were detected at S1 (all samples) and S3 (only the third monthly recruitment samples) near aquaculture farms, respectively. The anemone *Viatrix globulifera* (currently considered a synonym of *Bunodeopsis globulifera*) has been detected in sheltered area from previous studies, but the factors affecting its accumulation have been less studied (Fletcher et al. 2023). Detecting the presence of cnidarians is particularly important as several species have been implicated in causing negative outcomes for animal welfare and productivity on salmon farms (Fletcher et al. 2023). Detections such as this illustrates how fine-scale analysis of spatial and temporal settlement patterns can potentially be utilised to refine management approaches and the timing of interventions such as cleaning. In terms of the caprellid amphipods, we found rapid and potentially displacing growths occurred on both clean mesh and developed biofouling structures, indicating this might be driven by relevant feeding or competitive behaviours (Guerra-García and Tierno de Figueroa 2009).

Putatively non-native and aquaculture-relevant risk taxa

Interestingly, the three most dominant species detected in this study, represented by ASVs assigned to *Jassa slatteryi*, *Obelia geniculata*, and *Coryne eximia*, are all non-native to New Zealand (Zaiko et al. 2023). The predominance of non-native taxa in fouling communities aligns with observations from other temperate regions, where non-native species often contribute substantially to fouling assemblages on artificial structures (Azevedo et al. 2020; Leclerc et al. 2020). In aquaculture settings, fouling development and routine cleaning activities may further facilitate the local dispersal of non-native propagules (Floerl et al. 2016). Besides accumulating large biomass on aquaculture infrastructure, the hydroid species have been reported to negatively affect commercial kelp and salmon species by overgrowing on surfaces and spreading pathogens (Park and Hwang 2012; Kintner and Brierley 2019). The filamentous green algae (*Cladophora ruchingeri*) found at sheltered sites has also been considered a problematic species for blocking farming and harvesting equipment and resource competition with native mussels (Pochon et al. 2015; Cahill et al. 2022).

Apart from this, several potentially harmful native taxa were detected. ASVs assigned to a turbellarian flatworm species (*Notoplana australis,* Rhabditophora) were mostly detected at sheltered sites, particularly in summer. This species has previously been associated with weakened oysters and may pose risks to other mollusc species (Lester 1989). Although no documented negative impacts on aquaculture were found for ASVs assigned to the dominant turtle grass anemone species (*Viatrix globulifera*) detected at S1, it possesses cnidocytes (stinging cells) that can cause nerve irritation in humans (Burke 2002).

Potential future industry applications

A detailed understanding of biofouling dynamics across environmental gradients, together with the

identification of high-risk taxa, can support more targeted antifouling strategies (Bannister et al. 2019). This is particularly important in marine industries, where early prediction and prevention are generally more effective than post-settlement treatments (Fitridge et al. 2012). Furthermore, variability of biofouling settlement is often underestimated, highlighting the need of finer-scale, long-term monitoring using effective tools. The season- and exposure-associated patterns observed here suggest that management approaches may need to be tailored to local hydrodynamic conditions and dominant fouling community (Portas et al. 2023). At exposed sites, where biofouling communities and biomass exhibited stronger seasonal variability, approaches such as the use of durable, smooth-surfaced materials (e.g. nano-hybrid or composite coatings) combined with proactive and frequent cleaning could help reduce early biofilm formation and subsequent hydroid settlement, particularly in winter (Somya et al. 2024). Non-contact technologies, including ultrasonic antifouling systems (e.g. NetWave) or hydraulic cavitation tools (Zeytin et al. 2021; Yuan et al. 2023), may offer operational advantages for loosely attached fouling assemblages, although their effectiveness is likely to be site- and taxa-specific and warrants further evaluation. At sheltered sites with lower seasonal variability, consistent fouling management throughout the year may be more cost-effective, although optimising strategies for higher biodiversity and potential presence of high-risk fouling taxa may still be necessary. Factors not addressed here, such as anthropogenic influences and larval supply distribution, need to be further explored to explain community variation within similar season and exposure (Pineda et al. 2007).

Methodological considerations and future work

Metabarcoding enabled high-resolution detection of eukaryotic biofouling taxa and efficient community-level assessment compared to traditional morphology-based surveys (Taberlet et al. 2012). However, taxonomic assignments derived from metabarcoding represent putative molecular identifications and were not independently validated here, although complementary morphological studies have been completed (Tian et al. In prep). Community DNA extracted from homogenised samples may include DNA from other sources such as planktonic stages or adjacent benthic organisms, potentially over-representing the true mesh community. In addition, the use of 18S rRNA universal primers can limit species-level resolution and introduce risks of false positives, false negatives, and cross-contamination (Hadziavdic et al. 2014). For instance, sequences assigned to the Chilean shore crab *Cyclograpsus cinereus* at exposed sites may instead represent a closely related smooth shore crab *Cyclograpsus lavauxi* native to New Zealand and the only known *Cyclograpsus* species in the South Island. This is because there are currently no 18S rRNA gene sequences for *Cyclograpsus lavauxi* in publicly available reference databases (only one 16S rRNA mitochondrial gene sequence; GenBank accession AB440191.1), meaning any 18S reads from this species could match with other *Cyclograpsus* species. Similarly, the absence of previously reported pest species such as *Mytilus galloprovincialis* and *Undaria pinnatifida* at sheltered sites (Watts et al. 2015; Atalah et al. 2020), may reflect primer bias, low read abundance, or incomplete reference databases rather than true ecological absence.

While metabarcoding is a powerful tool for diversity and presence-absence assessments, it is less reliable for quantifying biomass or absolute abundance due to amplification and library preparation biases (Lamb et al. 2019). Although we included WW and DW measurements to estimate biomass, DW data were based on freeze-dried samples, which may retain residual moisture, and such physical quantification is challenging to apply on operational marine structures, underscoring the need for complementary, scalable quantification tools.

For future biofouling monitoring in marine environments, integrating metabarcoding with complementary quantification and validation tools, such as morphological surveys with standardised and automated image analysis, is likely to become a trend for rapid and effective community assessment (Gormley et al. 2018; Casey et al. 2021). The cost of biofouling management could be substantially reduced if monitoring facilitates preventative antifouling applications, and/or improves the timing and efficacy of post-settlement interventions such as physical removal (Bannister et al. 2019). Expanding monitoring to other critical biofouling groups, such as diatoms and bacteria, may explain the eukaryotic biofouling patterns in this study. Beyond prevention and mitigation, biofouling biomass may also be utilized by extracting chemical and nutrient components for value-added products, such as aquafeeds or medical materials. Alternatively, biofouling could potentially be used to facilitate contamination or nutrient remediation in restorative aquaculture and provide income to offset management costs (Zettler et al. 2013; Blunt et al.

2018). Biofouling management is not a simple process of organism removal, nor is there a single universal solution; effective management requires targeted, context-dependent strategies that balance ecological understanding with operational feasibility to support sustainable marine industries and ecosystem health (Cahill et al. 2022).

Conclusion

This study shows that seasonal and regional variations are associated with differences in biofouling community structure and biomass on mesh substrate. Using mesh material provided a realistic insight into fouling dynamics on industry-relevant substrates. Exposed sites exhibited strong seasonal shifts, with dense hydroid assemblages in winter and more diffuse, amphipod-dominated communities in summer. Sheltered sites showed more stable biomass and higher species richness, with notable site-specific variability suggesting additional local factors. These results underscore the need for context-specific antifouling strategies that consider both localised environmental conditions and material type. DNA metabarcoding proved effective for characterising eukaryotic biofouling communities, although limitations in quantification and primer specificity highlight the value of integrating complementary methods. Overall, this research informs targeted management approaches for marine industries and supports more sustainable biofouling mitigation practices.

Acknowledgements

This research was funded by the Bioeconomy Science Institute's (BSI's) Strategic Science Investment Fund (SSIF) Growing Futures investment. We thank Ulla von Ammon and Michelle Scriver from Cawthron Institute for the valuable discussions for experimental design and bioinformatic analyses. Igor Ruza, Belinda Timms, Benie Chambers and Glen Aspin from Bioeconomy Science Institute for the help with field trips and lab work, and Sequench Ltd. for sequencing advice.

Author contributions

CRediT: **Tian Tian**: Conceptualization, Data curation, Formal analysis, Investigation, Methodology, Project administration, Resources, Software, Validation, Visualization, Writing – original draft; **Xavier Pochon**: Conceptualization, Methodology, Resources, Supervision, Writing – review & editing; **Peter Bell**: Conceptualization, Funding acquisition, Investigation, Methodology, Project administration, Resources, Supervision, Writing – review & editing; **Maren Wellenreuther**: Conceptualization, Funding acquisition, Project administration, Supervision, Writing – review & editing.

Disclosure statement

No potential conflict of interest was reported by the author(s).

Funding

This research was funded by Plant & Food Research's SSIF Growing Futures investment.

ORCID

Tian Tian http://orcid.org/0009-0001-1533-3233
Xavier Pochon http://orcid.org/0000-0001-9510-0407
Maren Wellenreuther http://orcid.org/0000-0002-2764-8291

References

Akaike H. 1998. Information theory and an extension of the maximum likelihood principle. In: Parzen E, Tanabe K, Kitagawa G, editors. Selected papers of Hirotugu Akaike. Springer New York. p 199–213. https://doi.org/10.1007/978-1-4612-1694-0_15

Atalah J, Fletcher LM, Davidson IC, South PM, Forrest BM. 2020. Artificial habitat and biofouling species distributions in an aquaculture seascape. Aquacult Environ Interact. 12:495–509. https://doi.org/10.3354/aei00380

Atalah J et al. 2016. Preliminary assessment of biofouling on offshore mussel farms. J World Aquaculture Soc. 47(3):376–386. https://doi.org/10.1111/jwas.12279

Atalah J, Rabel H, Forrest BM. 2017. Modelling long-term recruitment patterns of blue mussels *Mytilus galloprovincialis*: a biofouling pest of green-lipped mussel aquaculture in New Zealand. Aquacult Environ Interact. 9:103–114. https://doi.org/10.3354/aei00216

Audrézet F et al. 2022. Eco-plastics in the sea: succession of micro- and macro-fouling on a biodegradable polymer augmented with oyster shell. Front Mar Sci. 9:891183. https://doi.org/10.3389/fmars.2022.891183

Azevedo J et al. 2020. Monitoring of biofouling communities in a Portuguese port using a combined morphological and metabarcoding approach. Sci Rep. 10(1):13461. https://doi.org/10.1038/s41598-020-70307-4

Bannister J, Sievers M, Bush F, Bloecher N. 2019. Biofouling in marine aquaculture: a review of recent research and developments. Biofouling. 35(6):631–648. https://doi.org/10.1080/08927014.2019.1640214

Bates D, Mächler M, Bolker B, Walker S. 2015. Fitting linear mixed-effects models using lme4. J Stat Soft. 67(1):1–48. https://doi.org/10.18637/jss.v067.i01

Beermann J, Franke HD. 2012. Differences in resource utilisation and behaviour between coexisting *Jassa* species (Crustacea, Amphipoda). Mar Biol. 159(5):951–957. https://doi.org/10.1007/s00227-011-1872-7

Behjati S, Tarpey PS. 2013. What is next generation sequencing? Arch Dis Child Educ Pract Ed. 98(6):236–238. https://doi.org/10.1136/archdischild-2013-304340
BioRender. 2025. BioRender: scientific figure and diagram tool. https://www.biorender.com
Blunt JW et al. 2018. Marine natural products. Nat Prod Rep. 35(1):8–53. https://doi.org/10.1039/c7np00052a
Braby CE, Somero GN. 2006. Ecological gradients and relative abundance of native (*Mytilus trossulus*) and invasive (*Mytilus galloprovincialis*) blue mussels in the California hybrid zone. Mar Biol. 148(6):1249–1262. https://doi.org/10.1007/s00227-005-0177-0
Burke WA. 2002. Cnidarians and human skin. Dermatol Ther. 15(1):18–25. https://doi.org/10.1046/j.1529-8019.2002.01508.x
Burnham KP, Anderson DR. 2002. Advanced issues and deeper insights. In: Burnham KP, Anderson DR, editors. Model selection and multimodel inference: a practical information-theoretic approach. Springer. p 267–351. https://doi.org/10.1007/978-0-387-22456-5_6
Cahill PL, Davidson IC, Atalah JA, Cornelisen C, Hopkins GA. 2022. Toward integrated pest management in bivalve aquaculture. Pest Manag Sci. 78(11):4427–4437. https://doi.org/10.1002/ps.7057
Callahan BJ et al. 2016. DADA2: high-resolution sample inference from Illumina amplicon data. Nat Methods. 13(7):581–583. https://doi.org/10.1038/nmeth.3869
Cao S, Wang JD, Chen HS, Chen DR. 2011. Progress of marine biofouling and antifouling technologies. Chin Sci Bull. 56(7):598–612. https://doi.org/10.1007/s11434-010-4158-4
Casey JM et al. 2021. DNA metabarcoding marker choice skews perception of marine eukaryotic biodiversity. Environ DNA. 3(6):1229–1246. https://doi.org/10.1002/edn3.245
Chan BKK, Chan WKS, Walker G. 2003. Patterns of biofilm succession on a sheltered rocky shore in Hong Kong. Biofouling. 19(6):371–380. https://doi.org/10.1080/08927010310001645229
Chiswell SM, Stevens CL, Macdonald HS, Grant BS, Price O. 2021. Circulation in Tasman-Golden bays and Greater Cook Strait, New Zealand. N Z J Mar Freshw Res. 55(1):223–248. https://doi.org/10.1080/00288330.2019.1698622
Clarke K, Green R. 1988. Statistical design and analysis for a "biological effects" study. Mar Ecol Prog Ser. 46:213–226. https://doi.org/10.3354/meps046213
ClipartMax. 2018. ClipartMax: free clipart images. https://www.clipartmax.com
de Souza VRS et al. 2025. Strategies for biofouling control: a review from an environmental perspective of innovation and trends. Coatings. 15(10):1185. https://doi.org/10.3390/coatings15101185
Dürr S, Thomason JC. 2009. Biofouling. Wiley-Blackwell.
Fitridge I, Dempster T, Guenther J, de Nys R. 2012. The impact and control of biofouling in marine aquaculture: a review. Biofouling. 28(7):649–669. https://doi.org/10.1080/08927014.2012.700478
Flemming HC, Murthy PS, Venkatesan R, Cooksey K. 2009. Marine and industrial biofouling. Springer.
Fletcher LM, Davidson IC, Bucknall BG, Atalah J. 2023. Salmon farm biofouling and potential health impacts to fish from stinging cnidarians. Aquaculture. 568:739315. https://doi.org/10.1016/j.aquaculture.2023.739315
Floerl O, Sunde L, Bloecher N. 2016. Potential environmental risks associated with biofouling management in salmon aquaculture. Aquacult Environ Interact. 8:407–417. https://doi.org/10.3354/aei00187
Fox J, Weisberg S. 2019. An R Companion to applied regression. Third edition. Sage.
Frerebeau N. 2025. Khroma: colour schemes for scientific data visualization. Université Bordeaux Montaigne. https://doi.org/10.5281/zenodo.1472077https://packages.tesselle.org/khroma/.
Garner YL, Litvaitis MK. 2013. Effects of wave exposure, temperature and epibiont fouling on byssal thread production and growth in the blue mussel, *Mytilus edulis*, in the Gulf of Maine. J Exp Mar Biol Ecol. 446:52–56. https://doi.org/10.1016/j.jembe.2013.05.001
Gormley K et al. 2018. Automated image analysis of offshore infrastructure marine biofouling. JMSE. 6(1):2. https://doi.org/10.3390/jmse6010002
Guerra-García JM, Tierno de Figueroa JM. 2009. What do caprellids (Crustacea: amphipoda) feed on? Mar Biol. 156(9):1881–1890. https://doi.org/10.1007/s00227-009-1220-3
Hadfield MG. 2011. Biofilms and marine invertebrate larvae: what bacteria produce that larvae use to choose settlement sites. Ann Rev Mar Sci. 3(1):453–470. https://doi.org/10.1146/annurev-marine-120709-142753
Hadziavdic K et al. 2014. Characterisation of the 18S rRNA gene for designing universal eukaryote specific primers. PLOS One. 9(2):e87624. https://doi.org/10.1371/journal.pone.0087624
Hartig F. 2025. DHARMa: residual diagnostics for hierarchical (multi-level/mixed) regression models. https://github.com/florianhartig/dharma
Kandlikar GS et al. 2018. Ranacapa: an R package and Shiny web app to explore environmental DNA data with exploratory statistics and interactive visualisations. F1000Res. 7:1734. https://doi.org/10.12688/f1000research.16680.1
Khosravi M, Nasrolahi A, Shokri MR, Dobretsov S, Pansch C. 2019. Impact of warming on biofouling communities in the northern Persian Gulf. J Therm Biol. 85:102403. https://doi.org/10.1016/j.jtherbio.2019.102403
Kintner A, Brierley AS. 2019. Cryptic hydrozoan blooms pose risks to gill health in farmed North Atlantic salmon (*Salmo salar*). J Mar Biol Ass. 99(2):539–550. https://doi.org/10.1017/S002531541800022X
Koehl MRA. 2007. Mini review: hydrodynamics of larval settlement into fouling communities. Biofouling. 23(5–6):357–368. https://doi.org/10.1080/08927010701492250
Kozich JJ, Westcott SL, Baxter NT, Highlander SK, Schloss PD. 2013. Development of a dual-index sequencing strategy and curation pipeline for analysing amplicon sequence data on the MiSeq Illumina sequencing platform. Appl Environ Microbiol. 79(17):5112–5120. https://doi.org/10.1128/AEM.01043-13
Kruskal JB. 1964. Multidimensional scaling by optimising goodness of fit to a nonmetric hypothesis. Psychometrika. 29(1):1–27. https://doi.org/10.1007/BF02289565

Lamb PD et al. 2019. How quantitative is metabarcoding: a meta-analytical approach. Mol Ecol. 28(2):420–430. https://doi.org/10.1111/mec.14920

Leclerc JC et al. 2020. Habitat type drives the distribution of non-indigenous species in fouling communities regardless of associated maritime traffic. Divers Distrib. 26(1):62–75. https://doi.org/10.1111/ddi.12997

Legendre P, Legendre L. 2012. Numerical ecology. Elsevier.

Lenth RV. 2025. Emmeans: estimated marginal means, aka least-squares means. https://cran.r-project.org/web/packages/emmeans/index.html

Lester RJG. 1989. Diseases of cultured molluscs in Australia. In: Aquacop, editor. Actes de Colloque. Proceedings of advances in tropical aquaculture workshop; 20 Feb-4 Mar; Tahiti, French Polynesia. French Institute for Ocean Science. p 207–216.

Lord JP. 2017. Temperature, space availability, and species assemblages impact competition in global fouling communities. Biol Invasions. 19(1):43–55. https://doi.org/10.1007/s10530-016-1262-7

Martin M. 2011. Cutadapt removes adapter sequences from high-throughput sequencing reads. EMBnet j. 17(1):10–12. https://doi.org/10.14806/ej.17.1.200

Martinez AP. 2020. PairwiseAdonis: pairwise multilevel comparison using adonis. https://github.com/pmartinezarbizu/pairwiseAdonis

McKnight DT et al. 2019. MicroDecon: a highly accurate read-subtraction tool for the post-sequencing removal of contamination in metabarcoding studies. Environ DNA. 1(1):14–25. https://doi.org/10.1002/edn3.11

McMurdie PJ, Holmes S. 2013. Phyloseq: an R package for reproducible interactive analysis and graphics of microbiome census data. PLOS One. 8(4):e61217. https://doi.org/10.1371/journal.pone.0061217]

Oksanen J et al. 2025. Vegan: community ecology package. https://cran.r-project.org/web/packages/vegan/index.html

Park CS, Hwang EK. 2012. Seasonality of epiphytic development of the hydroid *Obelia geniculata* on cultivated *Saccharina japonica* (Laminariaceae, Phaeophyta) in Korea. J Appl Phycol. 24(3):433–439. https://doi.org/10.1007/s10811-011-9755-3

Pearman JK et al. 2021. Metabarcoding as a tool to enhance marine surveillance of nonindigenous species in tropical harbours: a case study in Tahiti. Environ DNA. 3(1):173–189. https://doi.org/10.1002/edn3.154

Pineda J, Hare JA, Sponaugle S. 2007. Larval transport and dispersal in the coastal ocean and consequences for population connectivity. Oceanog. 20(3):22–39. https://doi.org/10.5670/oceanog.2007.27

Pochon X et al. 2015. *Cladophora ruchingeri* (C. Agardh) Kützing, 1845 (Cladophorales, Chlorophyta): a new biofouling pest of green-lipped mussel *Perna canaliculus* (Gmelin, 1791) farms in New Zealand. AI. 10(2):123–133. https://doi.org/10.3391/ai.2015.10.2.01

Pochon X, Zaiko A, Hopkins GA, Banks JC, Wood SA. 2015. Early detection of eukaryotic communities from marine biofilm using high-throughput sequencing: an assessment of different sampling devices. Biofouling. 31(3):241–251. https://doi.org/10.1080/08927014.2015.1028923

Portas A et al. 2023. Impact of hydrodynamics on community structure and metabolic production of marine biofouling formed in a highly energetic estuary. Mar Environ Res. 192:106241. https://doi.org/10.1016/j.marenvres.2023.106241

Puce S, Bavestrello G, Azzini F, Cerrano C. 2003. On the occurrence of *Coryne eximia* Allman (Cnidaria, Corynidae) in the Mediterranean Sea. Ital J Zool. 70(3):249–252. https://doi.org/10.1080/11250000309356525

Ruppert KM, Kline RJ, Rahman MS. 2019. Past, present, and future perspectives of environmental DNA (eDNA) metabarcoding: a systematic review in methods, monitoring, and applications of global eDNA. Glob Ecol Conserv. 17:e00547. https://doi.org/10.1016/j.gecco.2019.e00547

Seers B. 2018. FetchR: calculate wind fetch in R. https://cran.r-project.org/src/contrib/Archive/fetchR/

Sievers M, Dempster T, Fitridge I, Keough MJ. 2014. Monitoring biofouling communities could reduce impacts to mussel aquaculture by allowing synchronisation of husbandry techniques with peaks in settlement. Biofouling. 30(2):203–212. https://doi.org/10.1080/08927014.2013.856888

Slobodov SA, Marfenin NN. 2004. Reproduction of the colonial hydroid *Obelia geniculata* (L., 1758) (Cnidaria, Hydrozoa) in the White Sea. Hydrobiologia. 530–531(1–3):383–388. https://doi.org/10.1007/s10750-004-2682-4

Somya A et al. 2024. Anti-fouling nano-hybrid/composite smart coatings with specific reference to marine applications. In: Kumar A, Thakur A, editors. Nano-hybrid smart coatings: advancements in industrial efficiency and corrosion resistance. American Chemical Society. p 205–226. https://doi.org/10.1021/bk-2024-1469.ch009

Sylvester F et al. 2011. Hull fouling as an invasion vector: can simple models explain a complex problem? J Appl Ecol. 48(2):415–423. https://doi.org/10.1111/j.1365-2664.2011.01957.x

Taberlet P, Coissac E, Pompanon F, Brochmann C, Willerslev E. 2012. Towards next-generation biodiversity assessment using DNA metabarcoding. Mol Ecol. 21(8):2045–2050. https://doi.org/10.1111/j.1365-294X.2012.05470.x

Taudière A. 2023. MiscMetabar: an R package to facilitate visualisation and reproducibility in metabarcoding analysis. JOSS. 8(92):6038. https://doi.org/10.21105/joss.06038

Tian T, Pochon X, Bell P, Ashton D, Wellenreuther M.. In prep. Integrating metabarcoding and machine learning image analysis for complementary marine biofouling monitoring [unpublished manuscript]. New Zealand Institute for Bioeconomy Science Limited.

Ulaski BP, Konar B. 2024. Seasonal and site-specific differences in biofouling communities on Pacific oyster mariculture farms. J Exp Mar Biol Ecol. 578:152031. https://doi.org/10.1016/j.jembe.2024.152031

Valentini A, Pompanon F, Taberlet P. 2009. DNA barcoding for ecologists. Trends Ecol Evol. 24(2):110–117. https://doi.org/10.1016/j.tree.2008.09.011

Vecteezy. 2025. Vecteezy: free and pro vector art. https://www.vecteezy.com

Vinagre PA, Simas T, Cruz E, Pinori E, Svenson J. 2020. Marine biofouling: a European database for the marine renewable energy sector. JMSE. 8(7):495. https://doi.org/10.3390/jmse8070495

Visch W, Nylund GM, Pavia H. 2020. Growth and biofouling in kelp aquaculture (*Saccharina latissima*): the effect of location and wave exposure. J Appl Phycol. 32(5): 3199–3209. https://doi.org/10.1007/s10811-020-02201-5

von Ammon U et al. 2018. The impact of artificial surfaces on marine bacterial and eukaryotic biofouling assemblages: a high-throughput sequencing analysis. Mar Environ Res. 133:57–66. https://doi.org/10.1016/j.marenvres.2017.12.003

Watts AM, Goldstien SJ, Hopkins GA. 2015. Characterising biofouling communities on mussel farms along an environmental gradient: a step towards improved risk management. Aquacult Environ Interact. 8:15–30. https://doi.org/10.3354/aei00159

Whittaker RH. 1960. Vegetation of the Siskiyou Mountains, Oregon and California. Ecol Monogr. 30(4):407–407. https://doi.org/10.2307/1948435

Wilkinson L. 2011. ggplot2: elegant graphics for data analysis by Wickham H. Biometrics. 67(2):678–679. https://doi.org/10.1111/j.1541-0420.2011.01616.x

Wrange AL et al. 2020. Monitoring biofouling as a management tool for reducing toxic antifouling practices in the Baltic Sea. J Environ Manage. 264:110447. https://doi.org/10.1016/j.jenvman.2020.110447

Wu D, Hua J, Chuang SY, Li J. 2023. Preventative biofouling monitoring technique for sustainable shipping. Sustainability. 15(7):6260. https://doi.org/10.3390/su15076260

Yilmaz P et al. 2014. The SILVA and "all-species living tree project (LTP)" taxonomic frameworks. Nucleic Acids Res. 42(Database issue):D643–D648. https://doi.org/10.1093/nar/gkt1209

Yuan TP et al. 2023. Aquaculture net cleaning with cavitation improves biofouling removal. Ocean Eng. 285(1):115241. https://doi.org/10.1016/j.oceaneng.2023.115241

Zaiko A et al. 2023. Pest alert tool-a web-based application for flagging species of concern in metabarcoding datasets. Nucleic Acids Res. 51(W1):W438–W442. https://doi.org/10.1093/nar/gkad364

Zettler ER, Mincer TJ, Amaral-Zettler LA. 2013. Life in the "plastisphere": microbial communities on plastic marine debris. Environ Sci Technol. 47(13):7137–7146. https://doi.org/10.1021/es401288x

Zeytin S et al. 2021, October 4–7. The application of ultrasound as cage antifouling method and its impact on European sea bass, *Dicentrarchus labrax*. Poster session presented at: EAS Aquaculture Europe 2021, International Conference and Exposition; Madeira, Portugal.

Zhan A, Briski E, Bock DG, Ghabooli S, MacIsaac HJ. 2015. Ascidians as models for studying invasion success. Mar Biol. 162(12):2449–2470. https://doi.org/10.1007/s00227-015-2734-5

Zhan A et al. 2013. High sensitivity of 454 pyrosequencing for detection of rare species in aquatic communities. Methods Ecol Evol. 4(6):558–565. https://doi.org/10.1111/2041-210X.12037